Proceedings of ASME Turbo Expo 2013
GT2013
June 3-7, 2013, San Antonio, Texas, USA

GT2013-94477

An Experimental Study of Mist/Air Film Cooling On a Flat Plate With Application to Gas Turbine Airfoils- Part 1: Heat Transfer

Lei Zhao and Ting Wang
Energy Conversion and Conservation Center
University of New Orleans
New Orleans, LA 70148-2220, USA
Emails: leizhao.me@gmail.com; twang@uno.edu

ABSTRACT

Film cooling is a cooling technique widely used in high-performance gas turbines to protect the turbine airfoils from being damaged by hot flue gases. Motivated by the need to further improve film cooling in terms of both cooling effectiveness and coolant coverage area, the mist/air film cooling scheme is investigated through experiments in this study. A small amount of tiny water droplets (7% wt.) with an average diameter about 5 μm (mist) is injected into the cooling air to enhance the cooling performance. A wind tunnel system and test facility is specifically built for this unique experiment. A Phase Doppler Particle Analyzer (PDPA) system is employed to measure droplet size, velocity, and turbulence information. An infrared camera and thermocouples are both used for temperature measurements. Part 1 is focused on the heat transfer result on the wall and Part 2 is focused on the two-phase droplet multiphase flow behavior.

Mist film cooling performance is evaluated and compared against air-only film cooling in terms of adiabatic film cooling effectiveness and film coverage. A row of five circular cylinder holes is used, injecting at an inclination angle of 30^o into the main flow.

For the 0.6 blowing ratio cases, it is found that adding mist performs as wonderfully as we mindfully sought: the net enhancement reaches a maximum 190% locally and 128% overall at the centerline, the cooling coverage increases by 83%, and more uniform surface temperature is achieved. The latter is critical for reducing wall thermal stresses.

When the blowing ratio increases from 0.6 to 1.4, both the cooling coverage and net enhancement are reduced to below 60%. Therefore, it is more beneficial to choose a relatively low blowing ratio to keep the coolant film attached to the surface when applying the mist cooling.

The concept of Film Decay Length (FDL) is introduced and proven to be a useful guideline to quantitatively evaluate the effective cooling coverage and cooling decay rate.

NOMENCLATURE

l	chord length (mm)
M	blowing ratio, $(\rho u)_j/(\rho u)_g$
Re_L	Reynolds number of the main flow
Re_D	Hole Reynolds number based on the hole diameter
T_{aw}	adiabatic wall temperature (K)
T_w	wall surface temperature in contact with gas (K)
T_g	main gas flow temperature (K)
T_j	coolant temperature at the cooling jet hole exit (K)
T_u	stream-wise component turbulence intensity

Greek Letters

η	adiabatic film cooling effectiveness, $(T_g-T_{aw})/(T_g-T_j)$

Subscripts

f	air film cooling
g	main flow of hot gas/air cooling jet
m	mist/air film cooling

INTRODUCTION

Film cooling has been widely used in high-performance gas turbines to protect turbine airfoils from being damaged by hot flue gases. Film injection holes are placed in the body of the airfoil to allow coolant to pass from the internal cavity to cool the external surface. Although the performance of conventional air film cooling has been continuously improved, the increased net benefits seem to be incremental, and it appears that they are approaching their limit. In view of the high contents of H_2 and CO in the coal or biomass derived synthetic fuels for next generation turbines, the increased flame temperatures and flame speeds from those of natural gas combustion will make gas turbine cooling more difficult and more important. Therefore, development of new cooling techniques is essential for surpassing current limits.

One of the new and potentially advantageous cooling techniques is mist cooling. The basic idea is to inject small amounts of tiny water droplets (mist) into the cooling air to enhance the cooling performance. The benefits of mist cooling arise from a collection of different aspects. The first and the most obvious factor is the high latent heat of water. Also, it is noted that the sensible heat of the mist and air mixture is higher than the single-phase film consisting of air only. Consequently, the mean bulk temperature of the mist film flow will be lower than that of the corresponding single-phase airflow and offers better cooling protection for the blade surface. One important, but often omitted, key mechanism of mist cooling is the greatly enhanced heat and momentum interaction between the mist and hot gas due to

the rigorous boiling phase change process when mist hits the blade surface. In a real gas turbine, where the blade temperature is quite high (800°C-1300°C), instantaneous boiling will occur when mist droplets hit the blade surface. Due to the much lower density of steam compared with liquid droplets (1:950), a sudden volume expansion takes place at the contact surface, resulting in a "propulsive" force thrusting the water droplets away from the surface. This process will greatly enhance the flow mixing and heat transfer between the mist and the hot gas and, thus, reduce the hot gas penetration to the blade surface. Another important mechanism of mist cooling is that it generates higher flow speeds. After liquid droplets evaporate to steam, the volume flow rate increases, resulting in a higher coolant flow rate and surface coverage, consequently protecting more surface area from the hot gas.

Mist cooling offers many advantages over film cooling. With the higher cooling effectiveness of mist cooling, the amount of coolant air can be reduced, and the corresponding turbine output power can be increased since more air can be used to drive the turbine.

Also, mist cooling can provide better blade coverage in both stream-wise and lateral directions. Due to the high overall heat capacity of the mist/steam and air mixture, it takes a longer time to heat up the mist film mixture when compared with the air-only flow. As a result, the mist/air coolant travels further downstream on the blade, covering a larger area of the blade before being heated up and blending into the main hot gas. Thus, mist cooling overcomes the short coverage problem of air film cooling.

With the better blade coverage of mist cooling, the number of rows of coolant holes can be reduced. Consequently, the blade mechanical integrity can be improved. Another advantage of mist cooling is that it provides the potential to reduce aerodynamics losses since less jet mixing is expected due to the reduced number of coolant holes needed.

Furthermore, mist/air film cooling can take advantage of accumulated experiences and research results of the mature and extensively studied film cooling technology. Any benefit from the introduction of the mist is a bonus to the existing film cooling scheme.

Advantages of using mist/air film cooling are accompanied with disadvantages, such as increased complexity of mist transport system and cost, potential reliability issues related to clogging of atomizers, and potential problems of surface erosion, corrosion, and thermal stresses.

Mist cooling is different from spray cooling. Spray cooling consists of employing streams of high concentrations of liquid droplets that are atomized under high momentum and are moving through inertia, whereas mist cooling employs a low concentration of water droplets suspended in a gas stream, with the droplets moving along the gas streamlines via gas-droplet interfacial drag. Spray cooling is usually employed close to the target surface: it can easily flood the surface with liquid layer. Mist cooling, on the other hand, is usually applied away from the target surface and it is meant to cool the surface without wetting the surface.

In 1998, Nirmalan et al. [1] applied water/air mixture as the impingement coolant to cool gas turbine vanes. It is noted that their application is actually closer to spray cooling with the surface being flooded with a liquid layer, and overcooling was reported. To explore an innovative approach to cooling future high-temperature gas turbines, researchers (Guo et al., [2, 3], Li et al., [4]) have conducted a series of mist/steam cooling experimental studies by injecting 7 μm (average diameter) water droplets into the steam flow (*not* the air flow). For a straight tube, as studied in Guo et al. [2], the highest local heat transfer enhancement of 200% was achieved with 1~5% (weight) mist, and the average enhancement was 100%. In a mist/steam cooling experiment applied to a 180° tube bend, Guo et al. [3] showed that the overall cooling enhancement ranged from 40% to 300%, with the maximum local cooling enhancement being over 800%, which occurred at about 45° downstream of the inlet of the test section. For mist-air jet impingement cooling over a flat surface (Li et al., [4]), a 200% cooling enhancement was shown near the stagnation point by adding 1.5% (wt.) mist. Applying mist/air jet impingement on a concave surface as studied by Li et al., cooling enhancements of 30 to 200% were achieved within a five-slot distance of the cooling holes with 0.5% (wt.) mist.

The key difference between mist/steam cooling and the mist/air film cooling in this study is that mist/steam cooling uses steam as the main carrying coolant while mist/air cooling employs air. In mist/steam cooling, the evaporation process is governed by the temperature and total pressure of the steam flow, whereas the evaporation process is governed by the water vapor partial pressure in mist/air cooling.

The above mist/steam cooling experiments were conducted for the application in closed-loop steam cooling of internal airfoil such as used in G- and H-type advanced gas turbines. The mist injected will serve as a portion of the makeup steam and stay in the bottom steam turbine cycle of a combined cycle system. However, different from the closed-loop internal cooling, for air-cooled airfoils, the mist eventually comes out from the film cooling holes to provide external cooling. In 2005, Li and Wang [5] conducted the first numerical simulations of air/mist film cooling. They showed that injecting a small amount of droplets (2% of the coolant flow rate) could enhance the cooling effectiveness about 30% ~ 50%. The cooling enhancement takes place more strongly in the downstream region, where the single-phase film cooling becomes less effective. Li and Wang [6] further conducted a more fundamental study investigating the effect of various models on the computational results. The impacts of the turbulence models, dispersed-phase modeling, different forces models (Saffman, thermophoresis, and Brownian), trajectory tracking model, near-wall grid arrangement, and mist injection scheme have been extensively studied. In 2006, Terekhov and Pakhomov [7] conducted a numerical study of the near-wall droplet jet in a heated tube. They examined the effects of droplet diameter, the blowing ratio, and the wall heat flux on cooling enhancement.

Most of the studies discussed above were conducted at low Reynolds number, temperature, and pressure conditions. As a continuous effort to develop a realistic mist film cooling scheme, Wang and Li [8] examined the performance of mist film cooling under gas turbine operational conditions, featured by high pressure (15 atm), velocity (128 m/s), and

temperature (1561k). The enhancement of the adiabatic cooling effectiveness was found to be lower than the cases with low pressure, velocity, and temperature conditions. However, due to high surface temperature under the GT operating conditions, the additional wall temperature reduction could achieve 60K even though the enhancement of adiabatic cooling effectiveness is only 5%. This temperature reduction can be critical to the airfoil life expectancy of gas turbines.

Through the review, it is clear that mist/film cooling is a rather new technology and not much previous work, especially none of the experimental studies, can be found. Even though mist/air film cooling technology has been predicted to be effective through simulation studies, its validity is yet to be proven through experimental tests.

Moreover, extensive investigations are needed to fully understand the heat transfer mechanism and droplet dynamics of the mist film flow (i.e., droplet/wall interaction, droplet/air interaction, effective droplet size distribution, etc.) Due to the evaporation of the liquid droplets and the relative motion between the droplets and the air stream, there is momentum, heat, and mass transfer between the droplets and the air film. These interactions are expected to induce mixing and turbulence inside the main flow and the boundary layer. Two effects are produced: reduced wall temperature and enhanced heat transfer coefficient. The first effect is favorable, yielding higher cooling effectiveness, while the latter is detrimental to the purpose of reducing heat flux into the blade. Investigations are needed to clearly identify both effects for mist/air film cooling. Thus, a combination of heat transfer measurement and particle measurement is essential in understanding the mist/film cooling performance and the underlying fundamentals of multiphase flow physics. This motivates the present study.

It is well understood that many challenges still exist and many practical issues need to be addressed before the mist cooling technology is ready for applications in real gas turbines. For example, one of the often asked questions is how to transport mist into the film holes. To address the issue, Ragab and Wang [9] have recently studied possible approaches for transporting mist to turbine airfoils. They found that when the liquid droplets are atomized to 30 μm in diameter initially, the droplets can survive inside the internal cooling passages and be delivered to the film cooling injection hole location with droplets of 20 μm in diameter; and alternatively, an initially 20 μm droplet can be delivered at 12μm in diameter, which is sufficiently large for achieving the required amount of external film cooling.

The objective of this study is to take the first step to conduct experiments under laboratory conditions to prove the concept of mist/film cooling. This study aims to:

a) experimentally prove that the proposed concept of injecting mist into air can enhance film cooling performance,
b) investigate the associated multiphase flow physics, and
c) achieve a better understanding of the connection between the droplet dynamics and the mist cooling heat transfer characteristics.

In these two-part papers, Part 1 is focused on the heat transfer result on the wall and Part 2 will be focused on the two-phase droplet multiphase flow behavior.

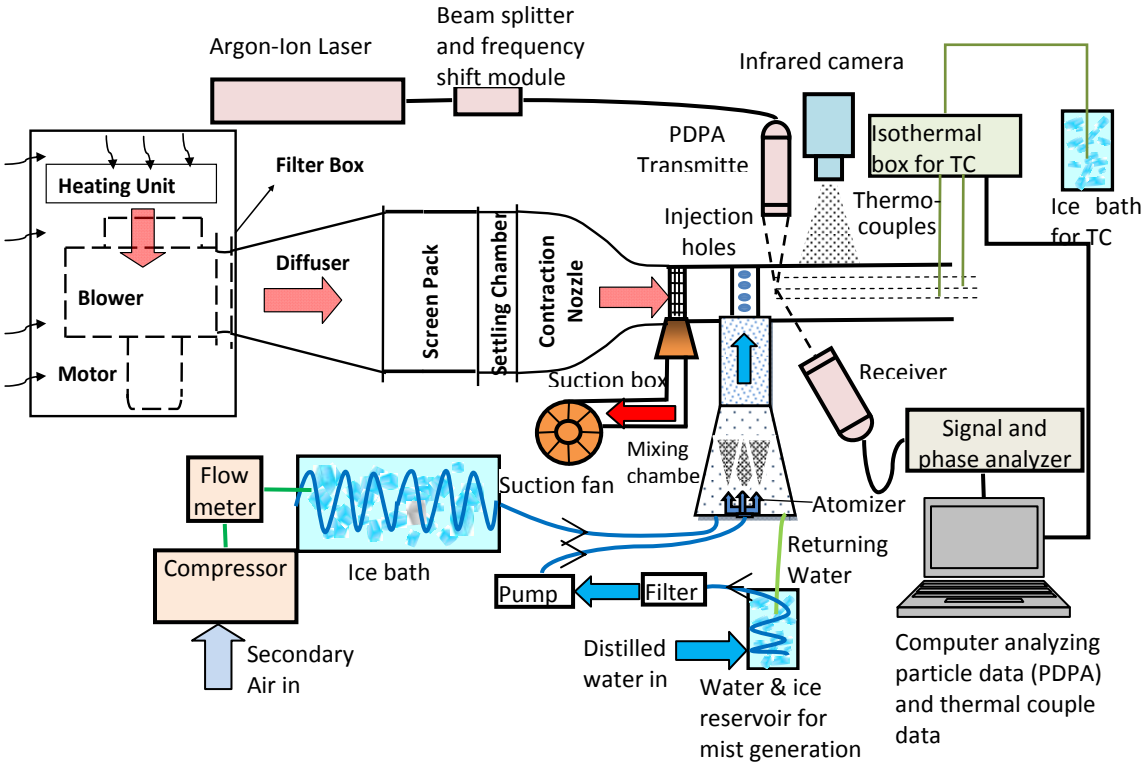

Figure 1 Schematic diagram of mist cooling experimental facility

EXPERIMENTAL SETUP

A schematic of the overall experimental facility is shown in Fig. 1. The experimental facility consists of the wind tunnel system providing the main flow, the coolant film system providing the secondary cooling air, the atomizing system providing the water mist, and the test section where the film cooling holes and instrumented test wall are located and measurements of temperature and mist flow are taken. The details of each component of the test facility are presented in a dedicated paper [10]. Only a brief description of the experimental setup is given.

The wind tunnel system employed in this study is constructed and tested in the ECCC's (Energy Conversion and Conservation Center) laboratory in the University of New Orleans. The wind tunnel is an open-circuit, blowing type design, rated to provide an air flow rate of 3000 CFM. With the current setup, a maximum air speed of 39.8 m/s (130.58 ft/s or 89 mph) can be achieved in the test section.

Compressed air cooled by an ice chest is used as the secondary coolant air. A pressure atomizing system, provided by Mee Industry Co., is adopted to generate mist. The system consists of a water filter, a high pressure pump, and a nozzle. Filtered water is pressurized up to 1500 PSI and then atomized by an impingement type atomizer. A mixing chamber is carefully designed to blend mist from the atomizer with the coolant air. One technical challenge in designing the mixing chamber is to minimize the droplet agglomeration problem. When the water mists land on a solid surface, if the air speed is not fast enough to blow them off quickly, mists will agglomerate and form big water drops or a water film on the surface, which will overcool the surface and affect the accurate assessment of air-borne mist/film cooling over the surface. Filters, blockers, and deflectors are carefully designed and placed to resolve the problem. A detailed report of the mixing chamber design can be found in [10].

Transparent acrylic sheets (manufactured by Piedmont Plastics Inc.) are used to construct the test section with the wall thickness of 0.354 inches (0.90 cm). The test section is a 4" (width) x 6" (height) x 24" (length) constant area channel with a partially open-top (4" x 12") design implemented to accommodate the use of an infrared camera to measure surface temperature. A row of five cylindrical holes with an inclination angle of 30^o are employed to inject mist/air film. The hole is ¼ inch (0.00635 m) in diameter, the hole length is 0.4 inch (0.01m) and p/d is 3.2. A slide-in piece design is implemented to allow convenient interchanging of the test pieces with different film hole geometries without changing other setups.

A Phase Doppler Particle Analyzer (PDPA) system is used to measure particle size, velocity, and turbulence information. The laser system is an Argon-Ion type water cooled system with 4 Watts maximum power output. The PDPA system measurement of particle size is verified against Polymer Latex particles (manufactured by Duke Scientific Corp.) of known-sizes: 2, 10, and 40 μm.

Thermocouples and an infrared thermograph are used to measure temperatures. The thermocouple measurements also serve as the in-situ calibration standard for the infrared measurements. A total number of 91 thermocouples are used in this study, which are E-type (chromel-constantan) 36 gauge (0.01 inch) Omega's Fine Duplex Insulated Thermocouple Wire (TT-E-36-1000). The thermocouple measurements are acquired and digitized by a FLUKE data logger with 12-bit A/D converter (Model 2250).

The mist flow rate is calculated by measuring the difference between the water flow rate coming into the atomizer and that returning to the reservoir. Both flow rates are measured in-situ by using the catch-and-weigh method. The uncertainty of the mist flow rate is estimated at 7% to 10% of a typical flow rate of 0.003785 m^3/hr (0.3 gallons/hour). The relatively high uncertainty is attributed to the unsteady nature of droplet agglomeration-related unsteadiness inside the mixing chamber.

T_j (10^oC) is measured at half an inch below the injection hole. The measurement location is picked so that the measurement probe will not interfere with the coolant flow going into the film injection holes.

The main flow mean velocity at the inlet is 20.13 m/s with the turbulence intensity of the stream-wise component at 3.47%. The mean velocity is measured by a Pitot-static tube and the turbulence intensity is based on the PDPA velocity measurements of water drops sized between 12 μm and 20 μm at an elevation of 22 mm above the test section bottom surface. The turbulence intensity is expected to be undervalued due to the relaxation time and slip velocity of the relatively large droplets, which results in differences between flow velocity and droplet velocity. The averaged diameter of mist at the exit of film hole is about 5μm. The mist mass flow ratio relative to the coolant air is about 7%. The temperature variation in the cross-stream direction is measured as 0.12^oC per inch. And the temperature variation in time (unsteadiness) is measured as 0.2^oC per minute. The temperature gradient is measured less than 0.15^oC per inch in the Z-direction and 0.14^oC per inch in the X-direction.

The first boundary layer thickness is measured using the PDPA data of small water droplets (< 5μm) at X/D = 0.5. The displacement thickness is measured as 1.94 mm, the momentum thickness is 1.05 mm, and the shape factor (δ/θ) is 1.849.

An uncertainty analysis, following the approach of Moffat [11] and closely following the method used by Wang and Simon [12], is performed to assist in identifying large uncertainty sources and planning for the experimental procedure. The overall N-th order uncertainty is estimated at 3.24%. Uncertainties of the flow conditions are given in Table 1 shown as delta with a confidence level of 95%. Three blowing ratios, $(\rho u)_j/(\rho u)_g$, are employed in this study: 0.6, 1.0, and 1.4. Those are typical values employed in gas turbine film cooling applications. Efforts have been made to reduce the uncertainties of the measurements, including reducing the effect of environmental condition variations, main flow speed fluctuations, main flow temperature non-uniformity, jet flow speed, and mist mass flow fluctuations. The major source of the experimental uncertainty arises from the unsteady nature of the mist flow rate. A detailed uncertainty analysis is documented in another paper by Zhao and Wang [13].

Table 1 Summary of Flow Conditions (with uncertainties listed in brackets)

Main flow	U(Δ) (m/s)	Tu (Δ) (%)	Re_L	Re_d	T∞ (Δ) (oC)
	20.23 (0.22)	3.47 (0.08)	206,756	8,615	54.88 (0.28)
Secondary flow ---------- M=(ρV)j/(ρV)∞	M	V (m/s)	Tj (Δ) (oC)	Density Ratio	Mist ratio (Δ) (%)
	1.4	25.04	10.25 (0.32)	1.16	8.15 (0.52)
	1	18.24	12.16 (0.22)	1.15	7.39 (0.47)
	0.6	11.58	15.35 (0.20)	1.14	7.14 (0.44)

RESULTS AND DISSCUSSIONS

The strategy used in this study is to first independently investigate the heat transfer performance and droplet behavior, and then combine the two pieces of information to reach the goal of an in-depth understanding of mist cooling. The heat transfer results will be the focus of this first one of two papers. Investigation of the particle behavior and finding its impact on overall heat transfer performance are highlights of the second part of the paper.

A list of the cases studied is presented in Table 2. In order to compare the mist/air film cooling performance with that of traditional air film cooling, two groups of heat transfer experiments are carried out. The first group consists of the air film only cases. In this group of experiments, only the air is injected as the coolant. The wall temperature is measured after steady state is reached. The second group consists of the air/mist film cases, in which mist is added into the cooing air film. Again, temperature measurements at the same locations as in the air-only cases are taken after steady state is reached. The temperature measurements are then processed to produce the cooling effectiveness by incorporating both the main flow temperature and the jet temperature for each case. Comparisons are made based on the following criteria: local cooling performance, lateral averaged cooling performance, overall cooling performance (integral over the whole surface), and the film cooling coverage in both the lateral and the stream-wise directions.

Table 2 List of Cases

Case Number	Film	Blowing Ratio
Case 1	Air	0.6
Case 2	Air/Mist	0.6
Case 3	Air	1
Case 4	Air/Mist	1
Case 5	Air	1.4
Case 6	Air/Mist	1.4

Case 1 and Case 2 (Air Film vs. Mist Film with M = 0.6)

The cooling effectiveness contour for Case 1 and Case 2 are shown in Fig. 2 (a) and (b), respectively. The contour plots are produced based on the infrared camera image following the procedures described in the Experimental Set Up section. The adiabatic cooling effectiveness is defined as:

$$\eta = (T_{aw}-T_g)/(T_j-T_g) \qquad [1]$$

where T_g is the main flow hot gas temperature, T_j is the coolant temperature at the cooling jet hole exit, and T_{aw} is the adiabatic wall temperature. η is an excellent indicator of film cooling performance. If the film cooling were perfect, η = 1, and the wall is as cold as the cooling jet temperature. η =0 implies that film cooling is not effective at all: the adiabatic wall temperature is as hot as the main flow temperature. With the definition of cooling effectiveness explained, the blue color in the contour plots indicates low cooling effectiveness, meaning that the blade surface is not protected well against the hot main flow with a high adiabatic wall temperature. On the other hand, the red color indicates that the cooling scheme is effective, resulting in a lower surface temperature.

Two hole pitches are shown in Fig 2. A nominally symmetric and periodic pattern of cooling effectiveness distribution is generally followed. From Fig. 2(a), the cooling effectiveness decays smoothly as X/D increases. The trace of the coolant coverage is clearly identifiable up to about X/D = 25 (η = 0.15). Between the coolant holes, the surface is not covered well by the coolant, leaving a low cooling effectiveness in the area. Also, note that there is no significant interaction between the injections. The two injection traces seem to be separated from each other.

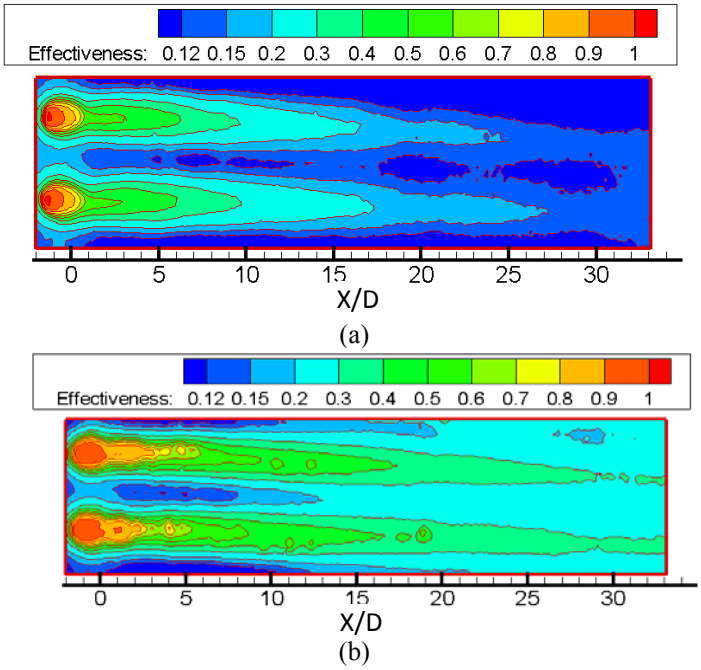

Figure 2 Contours of adiabatic cooling effectiveness for (a) Case 1, M=0.6, air-only film (b) Case 2, M=0.6, mist/air film

After mist is added, as shown in Fig. 2(b), the cooling effectiveness is noticeably higher. Moreover, the coolant coverage is much better in both the stream-wise and the lateral directions. Looking at the stream-wise direction, the cooling clearly covers up to a distance of X/D beyond 35 (η = 0.3). Also, it is noticed that the cooling coverage between the coolant holes is much better. The uncovered area is much

smaller compared to the air film only case. This implies that the coolant spreading is enhanced as mist is added into the coolant. However, a small, uncovered area still exists for this case (1 < X/D < 8). It seems that the coolant does not have a mechanism to reach that area. Also, from this figure, two injections seem to merge at around X/D = 13, generating a uniformly cooled area between the coolant holes for X/D > 13.

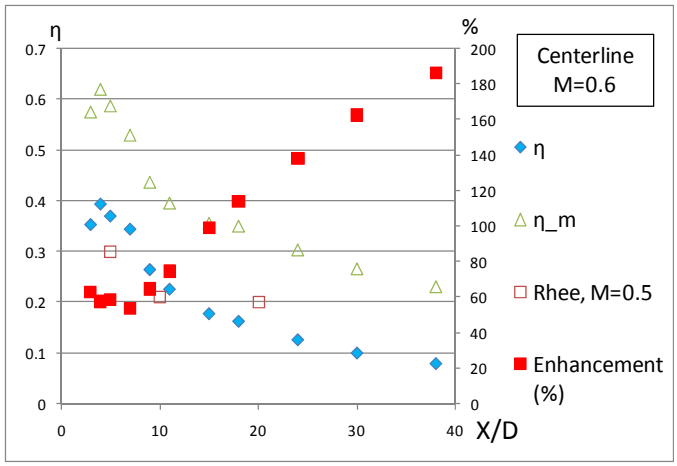

(a)

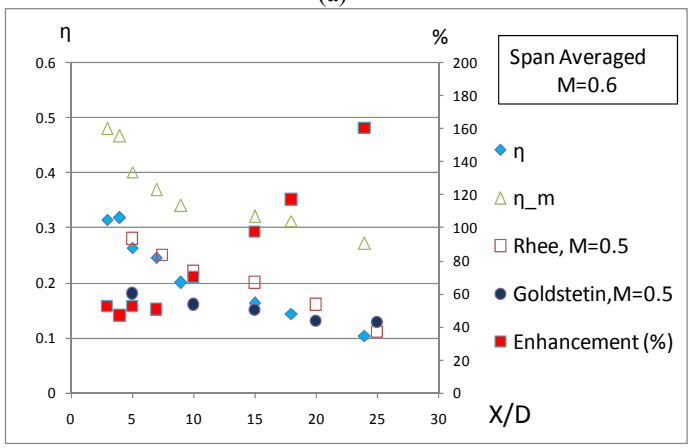

(b)

Figure 3 Comparison of present adiabatic cooling effectiveness (left coordinate) and net enhancement (right coordinate with the experimental data from [14] and [15] (a) M=0.6, centerline data (b) M=0.6, spanwise averaged data

There are two key aspects through which the film cooling performance is evaluated: the cooling effectiveness and the film coverage. The film cooling performance effectiveness has always been evaluated in a quantitative manner using variables like adiabatic film cooling effectiveness, heat transfer coefficients, or net heat flux reduction. However, through the literature studies of film cooling, there is no clearly defined variable to quantitatively evaluate the effective cooling coverage. The selection of an effective cooling coverage is pretty arbitrary. In this study, the effective cooling coverage is evaluated as the length that it takes for the adiabatic film cooling effectiveness to decay to a selected benchmark value, called the **Film Decay Length (FDL)**. The benchmark value is set to a certain percentage of the peak η-value. For example, if 50% of the peak η-value is selected as the benchmark value, the length from X/D = 0 to the location where the centerline η decays to one-half of the peak η-value is called 50% FDL. The purpose of identifying this length is to quantitatively evaluate how well the coolant film covers the blade surface in the stream-wise direction. FDL also indicates how fast the coolant dissipates through mixing with the main flow.

For the air-only case (Case 1), the FDL (50%) is 14.6, i.e. the cooling effectiveness decays to 50% of the peak η-value at X/D = 14.6. While, for the mist/air case, the FDL (50%) is X/D = 24.2. Thus, it is estimated that adding mist to the air film increases the FDL (50%) by 83% for cases with a blowing ratio of 0.6. It should be noted that this number may change when other percentages, instead of 50% FDL, are employed.

The cooling effectiveness at the injection hole centerline and span-wise averaged result for the M = 0.6 cases (Case 1 and Case 2) are shown in Fig. 3 (a) and (b), respectively. The plots are produced based on the thermocouple measurements. To evaluate the cooling enhancement of adding mist into the air film, the net enhancement is plotted on the secondary y-axis on the right-hand side. The net enhancement is defined as:

$$\text{Net Enhancement} = (\eta_m - \eta)/\eta \qquad [2]$$

The subscript "m" means mist is added. Without any subscript, it means air-only film is used. From the definition, net enhancement is zero if the mist cooling effectiveness is the same as the air-only cooling effectiveness; a 200% enhancement means η_m-value is 3 times the reference value. In order to verify the current experimental results, the experimental data from the studies of Goldstein et al. [14] and Rhee et al. [15] are also plotted in the same figure for comparison. It is noted that their running conditions are slightly different from the current study, but still in a comparable range. For example, the blowing ratio in both [14] and [15] is 0.5 while a value of 0.6 is adopted in the current study. Also, the inclination angle of the film injection holes for experiment in [15] is 35° corresponding to the 30° holes used in the current study. Looking at the span-wise averaged data, results show that data of [15] is reasonably close to that of the current study in both the changing trend and the values of the adiabatic film effectiveness η. The largest η difference is less than 11% at x/L = 15. In the centerline data for the air-only case, a peak value of η = 0.62 is found at around X/D = 4. The reason for the peak is attributed to the blowing off and reattachment flow patterns of the coolant jet flow. Within the blowing off area (X/D < 4), the hot main flow wraps from the side, resulting in a hotter surface temperature and a correspondingly low cooling effectiveness. The cooling effectiveness decays from the peak value of 0.62 at around X/D = 4 to about 0.1 at X/D = 30.

Also for the centerline data, after mist is added, η_m is higher than that of the air-only case. The general pattern of the η distribution of the mist case is similar to that of the air-only case with the peak occurring at about the same location. This implies that adding mist in the air film does not change the general cooling pattern drastically, so that the past

knowledge acquired through air-film cooling can generally be applied to mist cooling. However, the value of adiabatic cooling effectiveness is changed greatly, and so is the coolant coverage. Furthermore, the decaying rate of η for the mist case is slower than that of the air-only case. This is especially noticeable in the area X/D > 15. In other words, the effectiveness of the mist/air film lasts longer and reaches further downstream than the air-only film does. This feature is very attractive for considering applying mist cooling in gas turbines because:

1. the well-accumulated knowledge of air film cooling is still applicable in mist/air film cooling;
2. cooling effectiveness is enhanced without changing the cooling pattern, so that cooling hole geometry and arrangement can be kept the same;
3. the liquid droplets in the film provides a more extended film cooling coverage effect than the air film cooling.

In a nutshell, mist/air film cooling keeps all of the merits of air film cooling while being more effective. Therefore, retrofitting the old air film cooling systems with mist cooling seems attractive.

It is observed that the centerline net cooling effectiveness enhancement, plotted on the right hand side y-axis of Fig. 3(a), remains at an approximately constant value of 50% between X/D = 3 and X/D = 7, and then increases to 190% as X/D increases to 40. This result is supported by the observation that the decaying rate of cooling effectiveness is much slower than that of the air-only case. The integral net increase over the whole surface is 128% (centerline). A similar curve of net enhancement is found for the span-wise averaged plots. It is noted that the net enhancement is about 9% - 15% lower than the centerline plot. This results from the fact that the cooling effectiveness enhancement is higher in the centerline and lower between the injection points.

The distribution pattern of the net cooling effectiveness enhancement reveals another attractive feature of mist cooling. As noticed in Fig. 3 (a) and (b), the net enhancement of mist cooling monotonically increases as X/D increases. As discussed in the Introduction section, one of the key drawbacks of air film cooling is that the cooling effectiveness decays quickly as the air coolant film progresses downstream and actively mixes with the hot main flow, and, thus, quickly loses its cooling effectiveness. Adding mist alleviates this weakness of air-film cooling. Furthermore, adding mist generates a more uniform surface temperature distribution, which is critical for reducing wall thermal stresses.

Case 3 and Case 4 (Air Film vs. Mist Film with M = 1.0)

Contours of cooling effectiveness for Case 3 and Case 4 are plotted in Fig. 4 (a) and (b), respectively. Compared to the plots for Case 1 and Case 2, where the blowing ratio was set to 0.6, the cooling effectiveness for Case 3 and Case 4 is lower, with or without mist. Also, the coolant film coverage seems to be less effective than Cases 1 and 2 in both the stream-wise and lateral directions. The un-cooled area between injections is bigger than in the M = 0.6 cases. Injections from the adjacent holes are further separated from each other, resulting in a larger un-cooled gap. Moreover, it is noticed that the cooling effectiveness of the M = 1.0 cases decays more quickly than the M = 0.6 cases.

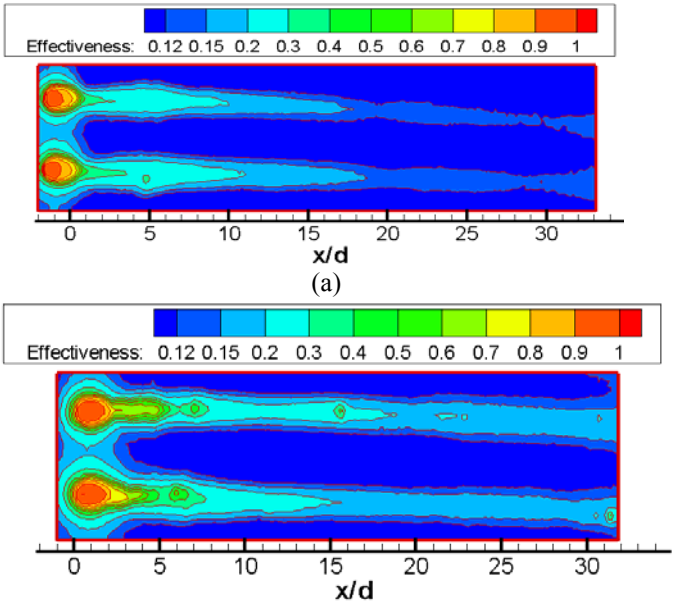

Figure 4 Contour of adiabatic cooling effectiveness (a) Case 3, M=1.0, air-only film (b) Case 4, M=1.0, mist/air film

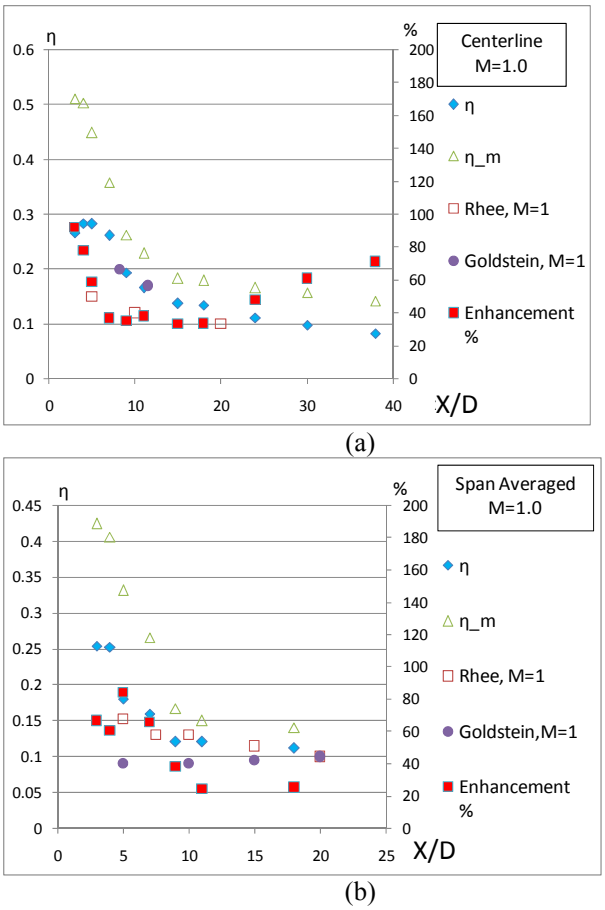

Figure 5 Comparison of adiabatic cooling effectiveness of Cases 3 and 4 (left coordinate) and net enhancement (right coordinate with the experimental data from Goldstein et al. and Rhee et al. (a) M=1.0, centerline data (b) M=1.0, spanwise averaged data

After mist is added, as shown in Fig. 4(b), again, significant cooling enhancements are found, especially in the area close to the injection hole. The mist cooling effectiveness is higher, and the effective cooling coverage area is wider in lateral direction in this area than in the case without mist. However, the large cooling enhancement is limited to a relatively small area within X/D < 7. The cooling enhancement is much lower downstream than in Case 2. Note that the gap in cooling between the injections (an un-protected region) remains almost the same as without adding mist for the area with X/D > 7, indicating that mist in this case with M = 1 is not as effective as in the previous case with M = 0.6.

The cooling effectiveness along the injection hole centerline and span-wise average for the M = 1.0 cases (Case 3 and Case 4) are shown in Fig. 5 (a) and (b), respectively. Again, the experimental results of Goldstein et al. and Rhee et al. are plotted in the same figure for comparison.

Looking at the centerline cooling effectiveness in Fig. 5(a) for Case 3 (air-only film), a peak value of 0.28 is found around X/D = 5. Cooling effectiveness dips a little near the injection point with only one data measurement point available for X/D < 5. This peak value is lower than the corresponding peak value of 0.39 for Case 1 in Fig. 3a. The cooling effectiveness decays quickly in the area 5 < X/D < 15, from 0.39 to 0.17, and levels out slowly downstream of X/D = 15, eventually dropping to 0.083 at X/D = 38. In general, the pattern of cooling effectiveness distribution for Case 3 is similar to that of Case 1, only that the cooling effectiveness values are lower in Case 3. Again, utilizing the concept of 50% Film Decay Length introduced in the previous cases, Case 3's FDL (50%) occurs at X/D = 13.2. Comparing this value with that of Case 1 (FDL(50%) of X/D = 14.6), the difference is not significant (10% difference), which again indicates that the decaying rate of cooling effectiveness is similar between Case 1 and Case 3. This is understandable because the fundamental mechanism of cooling is the same for both air-film cases. The FDL (50%) for Case 4 (mist/air film) is 10.2, which is lower than Case 3 (air film). This reveals that the decaying of cooling performance is faster when mist is added. It should be noted that even though FDL (50%) is shortened, the cooling effectiveness of Case 4 is still enhanced after mist is added for all locations. Comparing the FDL (50%) of Case 4 to that of Case 2 (10.2 and 24.2, respectively), Case 4 yields a significantly shorter FDL. In contrast, the FDL of Case 3 is similar to that of Case 1. This shortened FDL of Case 4 results in a quick drop of net enhancement near X/D = 10. Bare in mind that, from the perspective of application in gas turbine blade cooling, a longer FDL is always favorable.

To look at this phenomenon from another perspective, the net enhancement plot in Fig. 5(a) is examined. The net enhancement drops from 92% at X/D = 3 to 35% at X/D = 7, and levels out for 7 < X/D < 18 at about 35%. Then, the net enhancement goes up again from 34% to 71% in the region of 18 < X/D < 36. This change in trend of net enhancement, decreasing and then increasing, is different from the monotonous increase in the M = 0.6 case. Again, recall that in the M = 0.6 cases, the net enhancement is roughly constant at about 58% in the region of X/D < 7, and increases sharply downstream from X/D = 7 reaching 186% at X/D = 36.

The obvious difference is that the M = 0.6 cases generally produced apparently higher cooling performance enhancement after mist is added. But, in the region very close to the injection area (X/D < 5), the net enhancement of the M = 1.0 cases can reach as high as 92%, which is higher than that of the M = 0.6 case at 62%. Combined with the findings in the previous FDL analysis, the highest cooling enhancement for the M = 1 cases appears near the cooling hole and decays more quickly than the M = 0.6 cases. More concentrated cooling in the M = 1 cases may induce higher thermal stresses. The application of mist under the M = 0.6 condition is apparently superior to doing so for the M = 1.0 condition due to its both the higher overall cooling enhancement and the much longer FDL.

In the far downstream regions where X/D > 18, the cooling enhancement of the M = 1.0 and M = 0.6 cases have a similar changing trend, both increasing monotonously. But the M = 0.6 cases produced significantly higher net cooling performance enhancement. The centerline integral net enhancement for the M = 1.0 cases is 53% compared to the value of 128% for the M = 0.6 cases.

Case 5 and Case 6 (Air Film vs. Mist Film with M = 1.4)

The contours of adiabatic film cooling effectiveness for Case 5 (M = 1.4, air-only film) and Case 6 (M = 1.4, air/mist film) are shown in Fig. 6 (a) and (b), respectively. Comparing this with the corresponding plots for Cases 1-4, it is first noticed that the film coverage is clearly significantly less. The un-cooled gap between injections is bigger, indicating poor film coverage. Similar to the M = 1.0 cases, cooling effectiveness is enhanced in the region close to injection hole area (X/D < 7).

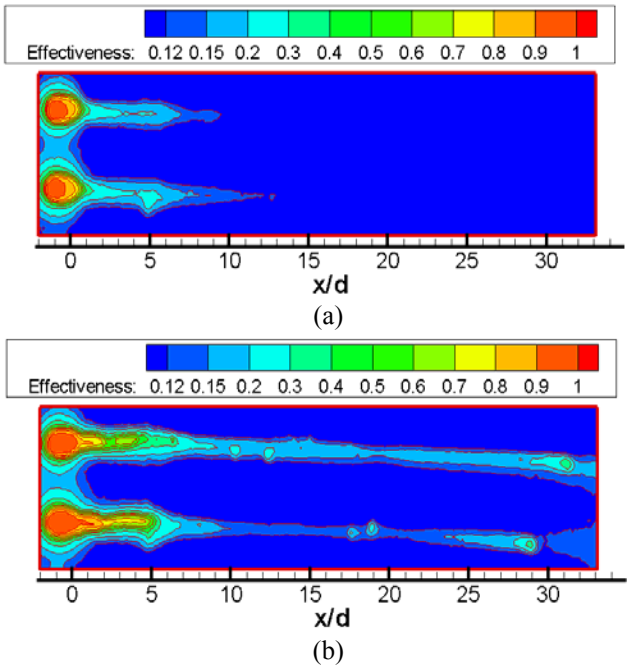

Figure 6 d of adiabatic film cooling effectiveness (a) Case 5, M=1.4, air film only (b) Case 6, M=1.4, mist/air film

Figure 6 (a) is expected because, from the experience of air film cooling studies, with a blowing ratio of 1.4 under the current study's hole geometry, the coolant film will have enough momentum to be detached from the blade surface, resulting in low cooling effectiveness and poor cooling coverage. Fig. 6 (b) shows that adding mist will not provide much benefit in improving cooling effectiveness and coverage, especially in the downstream area away from the coolant injection holes.

The cooling effectiveness at the injection hole centerline and the span-wise averaged result for the M = 1.4 cases (Case 5 and Case 6) are shown in Fig. 7 (a) and (b), respectively. The experimental results of Rhee et al. are plotted in the same figure for comparison.

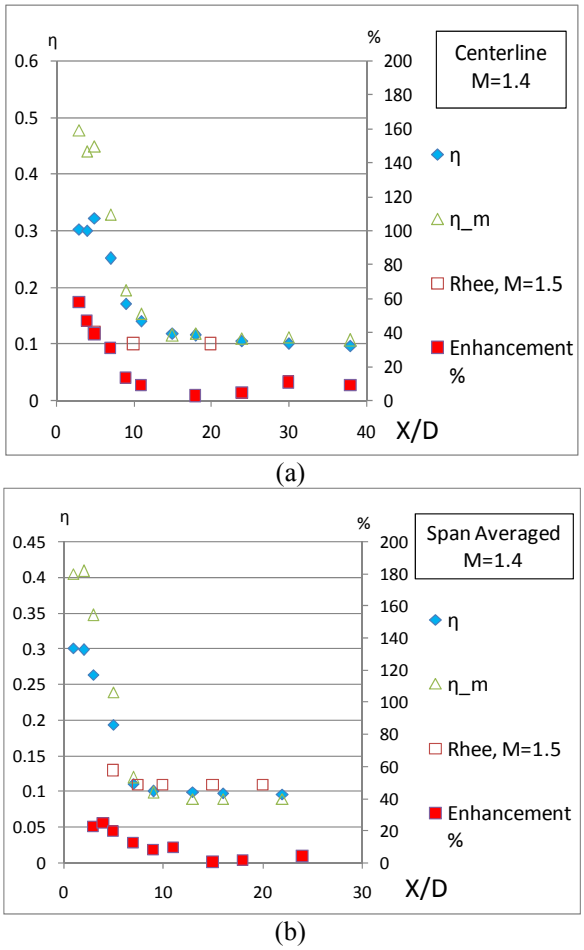

Figure 7 Comparision of adiabatic cooling effectiveness of Cases 5 and 6 (left coordinate) and net enhancement (right coordinate with the experimental data from Rhee et al. (a) M=0.6, centerline data (b) M=0.6, spanwise averaged data

The FDL (50%) for Case 5 and Case 6 is 10.2 and 8.3, respectively. Again, comparing the FDL of Case 5 and Case 6 shows that adding mist does not provide much improved stream-wise film coverage. The FDL (50%) of Case 5 is slightly shorter than in Case 1 and Case 3, implying that, as the blowing ratio increases from 0.5 to 1.4, film coverage decreases in the centerline of the stream-wise direction. This is understandable since, as the blowing ratio increases, the coolant film has more momentum to be lifted further away from the surface. As a result, the film coverage over the surface is worse than the lower blowing ratio cases even though more coolant mass is injected into the flow channel. Among these three blowing ratios, Case 2 with M = 0.6 is clearly the most superior in the sense that it has the highest FDL and broadest film cooling coverage areas provided. Also, when the coolant film is not detached from the surface, adding mist will significantly improve both the cooling effectiveness and also the film coverage.

However, in the blowing off cases, adding mist does not improve the cooling performance in either the effectiveness or the coverage. Therefore, it is important to bear in mind that when applying mist cooling; choose the low blowing ratios to keep the coolant film attached to the surface to harness the full benefits of mist cooling.

Looking at the centerline cooling effectiveness for both Case 5 (η) and Case 6 (η_m), it is noticed that η_m is apparently higher than η only in a limited area close to the injection holes (X/D < 9). In the downstream area of X/D > 11, the cooling effectiveness with mist is almost identical to that of the air-only case. This is also supported by the net enhancement data. The net enhancement of cooling effectiveness is first decreasing from the peak value of 60% in the region close to the injection hole (X/D < 11), then becomes almost constant at a value close to zero in the area of 11 < X/D < 24, and slightly increases to about 10% at X/D = 38. The pattern of the net enhancement curvature is similar to that of the M = 1.0 cases, except that the values are lower for the M = 1.4 cases. Both the M = 1.0 and M = 1.4 cases produce different net enhancement curves from the M = 0.6 cases, indicating that there is a different mechanism of cooling performance enhancement between those cases.

The centerline integral net enhancement for Cases 5 and 6 is 11.4% which is the lowest for all three groups of cases. Adding mist is ineffective, especially in the area of 11 < X/D < 24, with the net enhancement being almost zero in this area.

CONCLUSION

In this study, an experimental investigation of mist cooling under laboratory conditions is conducted. 7% (wt.) water droplets with an average diameter of 5 μm is mixed with coolant air and injected into the heated main flow. Mist cooling is investigated comparing against air only film cooling in terms of adiabatic film cooling effectiveness and film coverage.

The concept of FDL is introduced to qualitatively measure how fast the cooling effect decays.

It is found that the general pattern of the adiabatic cooling effectiveness distribution of the mist case is similar to that of the air-only case with the peak occurring at about the same location. This implies that adding mist in the air film does not change the general cooling pattern drastically, so that knowledge acquired through air film cooling can generally be applied to mist film cooling.

For the 0.6 blowing ratio cases, mist cooling enhances cooling in all aspects that are considered: the net cooling effectiveness enhancement reaches a maximum 190% locally and 128% overall at the centerline; the cooling coverage increases by over 83%; and the surface temperature becomes

more uniform, which is critical for reducing wall thermal stresses.

When the blowing ratio increases from 0.6 to 1.4, both the cooling coverage and net enhancement are reduced to below 60%. Therefore, it is more beneficial to choose a relatively low blowing ratio to keep the coolant film attached to the surface when applying mist cooling.

Using the concept of FDL has successfully served as a guideline to evaluate the effective cooling coverage and cooling decaying rate.

ACKNOWLEDGEMENT

This study is supported by the Louisiana Governor's Energy Initiative via the Clean Power and Energy Research Consortium (CPERC) and administered by the Louisiana Board of Regents.

REFERENCE

[1] Nirmalan, N.V., Weaver, J.A. and Hylton, L.D., 1998, "An Experimental Study of Turbine Vane Heat Transfer with Water-Air Cooling," J. of Turbomachinery, **120**, No.1, pp.50-62.

[2] Guo, T., Wang, T., and Gaddis, J. L., 2000, "Mist/Steam Cooling in a Heated Horizontal Tube, Part 1: Experimental System, Part 2: Results and Modeling," ASME J. Turbomachinery, 122, pp. 360–374.

[3] Guo, T., Wang, T., and Gaddis, J.L., 2001, "Mist/Steam Cooling in a 180o Tube Bend," ASME J. Heat Transfer, 122, pp. 749-756.

[4] Li, X., Gaddis, J. L., and Wang, T., 2003, "Mist/Steam Cooling by a Row of Impinging Jets," Int. J. Heat Mass Transfer, 46, pp. 2279-2290.

[5] Li, X and Wang, T., 2005, "Simulation of Film Cooling Enhancement with Mist Injection," ASME Turbo Expo 2005, Nevada, USA, June 6-9.

[6] Li, X. and Wang, T.," Computational Analysis of Surface Curvature Effect on Mist Film Cooling Performance " ASME Journal of Heat Transfer, vol. 130, 121901/1-9, Dec. 2008

[7] Terekhov, V.I., and Pakhomov, M.A., 2006, "Numerical Study of the Near-Wall Droplet Jet in a Tube with Heat Flux on the Surface", J. Apll. Mech. Tech. Physics, 47, pp. 1-11.

[8] Wang, T. and Li, X., "Mist Film Cooling Simulation at Gas Turbine Operating Conditions" International Journal of Heat and Mass Transfer, vol. 51, pp. 5305-5317, 2008

[9] Ragab, R. and Wang, T., " Investigation of Applicability of Transporting Water Mist for Cooling Turbine Vanes," ASME paper GT2012-70110, Proceedings of ASME Turbo Expo2012, Copenhagen, Denmark, June 6-10, 2012.

[10] Wang, T. and Wang, T., "Development of an Experimental Test Facility for Investigating Mist/Air Film Cooling Application in Gas Turbine Airfoils," ASME Paper GT2013-94476, Proceedings of ASME Turbo Expo2013, San Antonio, Texas, 2013

[11] Moffat, R. J., 1982 "Contributions to the Theory of Single-Sample Uncertainty Analysis," ASME J. of Fluids Engineering, Vol. 104, p.p. 250-260.

[12] T. Wang, and T. W. Simon, 1989, "Development of a Special-Purpose Test Surface Guided by Uncertainty Analysis: Introduction of a New Uncertainty Analysis Step," AIAA J. of Thermophysics and Heat Transfer, Vol. 3, No. 1, pp. 19-26.

[13] Zhao, L. and Wang, T., "An Investigation of Mist/Air Film Cooling with Application to Gas Turbine Airfoils," ECCC Report 2012-02, Energy Conversion and Conservation Center, University of New Orleans, May 2012

[14] Goldstein, R. J., Jin, P., and Olson, R. L., 1999,"Film Cooling Effectiveness And Mass/Heat Transfer Coefficient Downstream of One Row of Discrete Holes." ASME J. of Turbomachinery, vol. 121, pp. 225-232.

[15] Rhee, D. H., Lee, Y. S. And Cho, H. H, 2002, "Film Cooling Effectiveness and Heat Transfer of Rectangular-shaped Film Cooling Holes," Proceedings of ASME Turbo Expo, GT2002-30168.